

## RESEARCH LETTER

10.1029/2018GL077605

### Key Points:

- Sixty-two years (1954–2016) of aerial photography and radar data document recent acceleration of a rock glacier complex in northern Norway
- Results show spatial and temporal variations as extension and compression, uplift, and subsidence in a permafrost landform
- Simultaneous increase of temperature and precipitation suggests that the landform is affected by permafrost warming

### Supporting Information:

- Supporting Information S1
- Figure S1
- Figure S2
- Figure S3
- Figure S4
- Figure S5
- Figure S6
- Figure S7
- Figure S8
- Figure S9
- Figure S10
- Figure S11
- Figure S12
- Figure S13
- Figure S14
- Figure S15
- Data Set S1
- Data Set S2
- Movie S1
- Movie S2
- Movie S3
- Movie S4

### Correspondence to:

H. Ø. Eriksen,  
haraldoverlieriksen@gmail.com

### Citation:

Eriksen, H. Ø., Rouyet, L., Lauknes, T. R., Berthling, I., Isaksen, K., Hindberg, H., et al. (2018). Recent acceleration of a rock glacier complex, Adjet, Norway, documented by 62 years of remote sensing observations. *Geophysical Research Letters*, 45, 8314–8323. <https://doi.org/10.1029/2018GL077605>

Received 7 MAR 2018

Accepted 27 JUL 2018

Accepted article online 3 AUG 2018

Published online 23 AUG 2018

©2018. The Authors.

This is an open access article under the terms of the Creative Commons Attribution-NonCommercial-NoDerivs License, which permits use and distribution in any medium, provided the original work is properly cited, the use is non-commercial and no modifications or adaptations are made.

## Recent Acceleration of a Rock Glacier Complex, Adjet, Norway, Documented by 62 Years of Remote Sensing Observations

H. Ø. Eriksen<sup>1,2</sup> , L. Rouyet<sup>1</sup> , T. R. Lauknes<sup>1</sup> , I. Berthling<sup>3</sup> , K. Isaksen<sup>4</sup> , H. Hindberg<sup>1</sup> , Y. Larsen<sup>1</sup> , and G. D. Corner<sup>2</sup>

<sup>1</sup>Norut, Tromsø, Norway, <sup>2</sup>Department of Geosciences, UiT-The Arctic University of Norway, Tromsø, Norway, <sup>3</sup>Department of Geography, Norwegian University of Science and Technology, Trondheim, Norway, <sup>4</sup>Norwegian Meteorological Institute, Research and Development Department, Oslo, Norway

**Abstract** Recent acceleration of rock glaciers is well recognized in the European Alps, but similar behavior is hardly documented elsewhere. Also, the controlling factors are not fully understood. Here we provide evidence for acceleration of a rock glacier complex in northern Norway, from 62 years of remote sensing data. Average annual horizontal velocity measured by aerial feature tracking increased from  $\sim 0.5 \text{ myr}^{-1}$  (1954–1977) to  $\sim 3.6 \text{ myr}^{-1}$  (2006–2014). Measured by satellite synthetic aperture radar offset-tracking, averages increased from  $\sim 4.9$  to  $\sim 9.8 \text{ myr}^{-1}$  (2009–2016) and maximum velocities from  $\sim 12$  to  $\sim 69 \text{ myr}^{-1}$ . Kinematic analysis reveals different spatial-temporal trends in the upper and the lower parts of the rock glacier complex, suggesting progressive detachment of the faster front. We suggest that permafrost warming, topographic controls, and increased water access to deeper permafrost layers and internal shear zones can explain the kinematic behavior.

**Plain Language Summary** Using remote sensing data we document unusual high surface displacement and accelerations on a rock glacier complex in a mountain hillside in northern Norway. Increasing creep rates have been reported from the European Alps, but an acceleration of this order has not been documented in Scandinavia before. Rock glaciers are permafrost landforms consisting of a mix of ice and debris. Using aerial photos, we document an acceleration from  $\sim 0.5 \text{ m per year}$  (1954–1977) to  $\sim 3.6 \text{ m per year}$  (2006–2014) for the lower parts of the rock glacier complex. For the same area, we observe an increase from  $\sim 4.9$  to  $\sim 9.8 \text{ m per year}$ , measured by satellite-based radar between 2009 and 2016. Maximum velocities increased from  $\sim 12$  to  $\sim 69 \text{ m per year}$ . Results suggest that the fast lower part is detaching from the slower upper part. Radar data delineate areas with subsidence and uplift, compression, and extension. Increase in temperature and precipitation during the 62-year period indicates possible permafrost degradation. Our work demonstrates the value of combining remote sensing data sources in documenting permafrost landforms in the Arctic. Important work still remains to document and understand their evolution and the effects of climate change.

## 1. Introduction

Rock glaciers are striking landforms developed from deformation of ice/debris mixtures under permafrost conditions (Barsch, 1996; Berthling, 2011; Gorbunov et al., 1992; Haeberli et al., 2006). They form a common but not ubiquitous part of high alpine and polar slope systems. Ground temperature influences the rheology of such ice/debris mixtures in a nonlinear manner (Kääb et al., 2007; Moore, 2014), but rock glaciers also respond dynamically to changes in sediment input (Müller et al., 2016) and rain or snow-meltwater infiltration (Ikeda et al., 2008). For more than a decade, a significant acceleration, and in some cases even collapse, of rock glaciers has been documented in the European Alps (Avian et al., 2005; Bodin et al., 2016; Delaloye et al., 2008; Ikeda et al., 2008; Kääb et al., 2007; Kellerer-Pirklbauer & Kaufmann, 2018; Müller et al., 2016; Noetzli et al., 2016; Roer et al., 2008). This development has been attributed to higher permafrost temperatures (Kääb et al., 2007; Kellerer-Pirklbauer & Kaufmann, 2012; Roer et al., 2005) combined with increasing liquid water content (Ikeda et al., 2008; Kenner et al., 2017) and local overloading by debris (Delaloye et al., 2013). The factors controlling acceleration and complex velocity variations are not known in detail (Haeberli et al., 2010; Müller et al., 2016). Importantly, similar behaviors are still poorly documented outside the European Alps, except for work by Darrow et al. (2016, 2017), making the present work an important contribution to obtaining a global overview of accelerating permafrost landforms in the context of climate

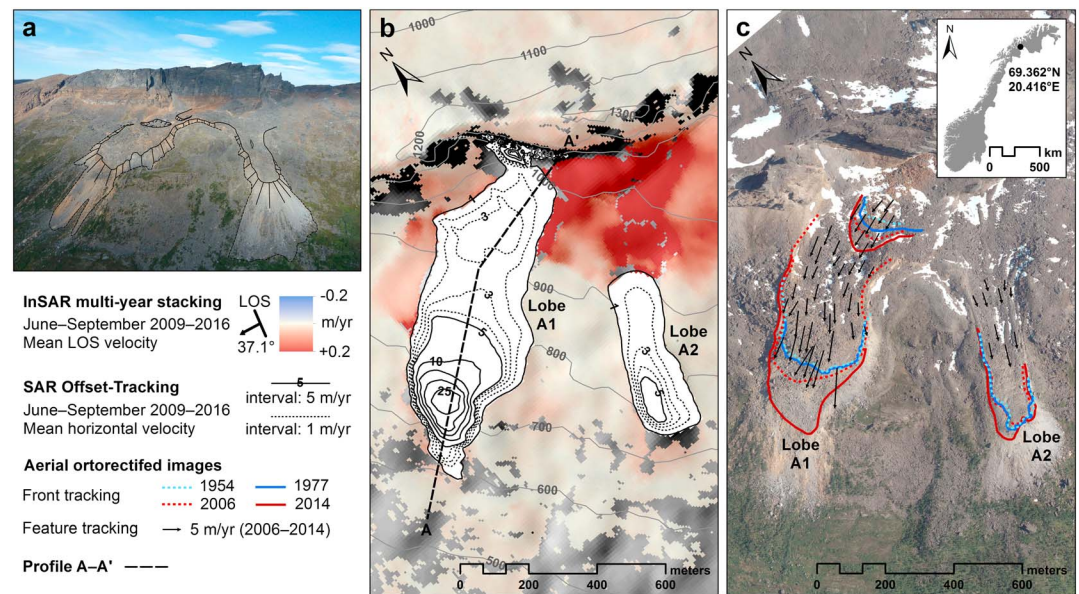


**Figure 1.** Spatial distribution of ground displacements in the rock glacier complex at the Ádjet mountain. (a) Aerial photo close-up of the two most active rock glacier lobes (NGU, 14 August 2011). (b) Mean annual ground velocities along the line-of-sight measured by InSAR multiyear stacking (2009–2016, minus 2015). The red areas indicate active slope processes with displacements away from the satellite (downward and westward). The contours on lobes, A1 and A2, indicate projected horizontal mean annual velocities ( $\text{myr}^{-1}$ ) detected using SAR offset-tracking (2009–2016, minus 2015). Background: shaded relief from 10-m resolution digital elevation model (Norwegian Mapping Authority, 2013). (c) Results from aerial feature- and front tracking in 1954, 1977, 2006, and 2014. Background: orthorectified image from 31 August 2014. Inset: location of the study area in northern Norway.

change. Over the last few decades, developing remote sensing techniques have complemented traditional in situ investigation and monitoring methods. Optical and radar sensors mounted on satellite, airborne, and ground-based platforms have proven especially suitable for measurement of deformation on rock glaciers (Kääb et al., 1997; Liu et al., 2013; Rignot et al., 2002; Wang et al., 2017).

The objective of this paper is to document and analyze spatiotemporal trends and changes of displacement rates over a fast-moving rock glacier complex in northern Norway by exploiting optical and radar remote sensing data sets spanning 62 years (1954–2016).

## 2. Ádjet Rock Glacier Complex, Northern Norway

Our study area is located in Troms County, northern Norway (Figure 1c inset), which has a high density of rockslides (Bunkholt et al., 2013; Corner, 2005; Lauknes et al., 2010; Osmundsen et al., 2009), and the highest density of rock glaciers in Norway (Lilleøren & Etzelmüller, 2011). We focus on a prominent rock glacier complex, composed of two lobes (A1 and A2), located below a summit reaching up to 1,300 m above sea level (asl), on the southwest-facing slope of Ádjet mountain in the Skibotn valley (Figure 1 and Figures S1 and S9 and Text S1 in the supporting information). Lobe A1 ranges in elevation from ~690 to 1,080 m asl (Figures 1, S1, S2, S9, S10, and S12), close to the regional altitudinal limit of mountain permafrost (600–800 m asl) according to borehole temperature data and modeling (Farbrot et al., 2013; Kellerer-Pirklbauer & Kaufmann, 2018). Scree aprons on the steep front of lobe A1 reach down to 580 m asl (Figures 1, S1, S2, and S10 and File S1 in the supporting information). The rock glaciers have developed from debris from rockslides and rockfalls accumulated below a ~200-m high, subvertical, and highly fractured headwall consisting of quartz-rich schist and garnet-mica-schist (Bakkhaug, 2015; Nopper, 2015). The lobes have longitudinal and transverse furrows, some with snow and perennial ice in the bottom. The deepest depression is ~16 m deep, located on the gently sloping middle part of lobe A1 (~880 m asl). On lobe A2, we observed during the summers 2015–2017, a thermokarst lake with bottom ice between large boulders (File S1).

### 3. Data and Methods

#### 3.1. Data

The study is based on four remote sensing data sets comprising (1) four orthorectified aerial images from 1954, 1977, 2006, and 2014; (2) 63 snow-free TerraSAR-X (TSX) satellite images, StripMap (SM) mode, in ascending geometry; (3) 75 snow-free TSX images, SM mode, in descending geometry; and (4) Gamma Portable Radar Interferometer images acquired during two campaigns in August 2014 and May–June 2015.

Remote sensing data sets are complemented with climatic data comprising (1) modeled air temperature, precipitation, and snow cover data from SeNorge.no portal, 2012 and (2) in situ air, ground surface, and ground temperature from iButton loggers (Eriksen, 2018).

Characteristics of remote sensing, modeled, and in situ data are summarized in Table S1 in the supporting information.

#### 3.2. Methods

The remote sensing techniques applied are (1) aerial feature- and front tracking based on the orthorectified aerial images; (2) SAR interferometry (InSAR) multiyear stacking based on TSX images in descending geometry; (3) SAR offset-tracking (OT) technique based on TSX images in ascending and descending geometries; and (4) Terrestrial InSAR (TRI) based on Gamma Portable Radar Interferometer images. As summarized in Table S2, the combination of these remote sensing methods is necessary to span over the whole time period (62 years from 1954 to 2014), detect ground displacements on both slow and fast moving areas, and document both long-term trend and seasonal variations. More information about each method is available in Texts S2a–S2d).

Offset-tracking and TRI results are projected using an assumption of displacements parallel to the surface and analyzed along a profile A-A' (Figures 1 and S2). Velocities from aerial feature- and front tracking, OT and TRI are compared by computing the mean annual horizontal velocity for a common area in the middle of lobe A1 (Figures S1 and S2). InSAR documents displacement rates in surrounding areas. TRI documents seasonal variations of rates by comparing results from summer 2014 and spring 2015. The kinematic analysis includes the calculation of the strain rate (extension/compression) and variations of uplift/subsidence trends, based on TRI and OT results (Text S2e).

The modeled climatic data are used to compute mean annual air temperature (MAAT), mean annual precipitation, and maximum annual snow depth (MASP). This provides a long temporal coverage (1957–2016) to investigate climate change in the region. For comparison with modeled data, we calculated MAAT based on in situ air temperature data. To characterize the ground thermal regime at local scale, mean annual ground surface and ground temperature are calculated. Using the Bottom Temperature of Snow (BTS) method (Haeberli, 1973; Hoelzle, 1992), stable temperatures during snow cover provide an indication of permafrost presence/absence at different locations. More information about climatic analysis is available in Text S2f.

### 4. Results

The results from the four complementary remote sensing methods document high velocities on the rock glacier complex, with fastest velocities located on lobe A1 (Figures 1b and 1c). Aerial feature- and front tracking shows that the lobe front of A1 advanced by ~180 m and one upper internal lobe front advanced by ~100 m between 1954 and 2014 (Figures 1c, S3, and S4). The front of lobe A2 advanced ~35 m during the same time span. Mean annual velocities from InSAR multiyear stacking show velocities up to  $0.15 \text{ myr}^{-1}$  along the LOS in the source area under the headwall supplying the rock glacier complex (Figures 1c and S1). Because of large displacements on lobes A1 and A2, InSAR fails to provide correct measurements (Text S2b). However, SAR offset-tracking is able to follow the displacement and documents 2009–2016 (minus 2015) mean annual velocities up to  $\sim 27 \text{ myr}^{-1}$  on lobe A1 and up to  $\sim 6 \text{ myr}^{-1}$  on lobe A2 (Text S2c), including a clear acceleration between 2009 and 2016 (Figures S6 and S7).

#### 4.1. Long-Term Trends

To compare the results, the surface-parallel flow approximation was used to project OT and TRI velocities in the downslope direction, using a profile along the fastest lobe A1 (Figures 1 and S2). Figure 2a shows velocities from each year separately along the profile A-A'. OT results for 2016 show a maximum surface-

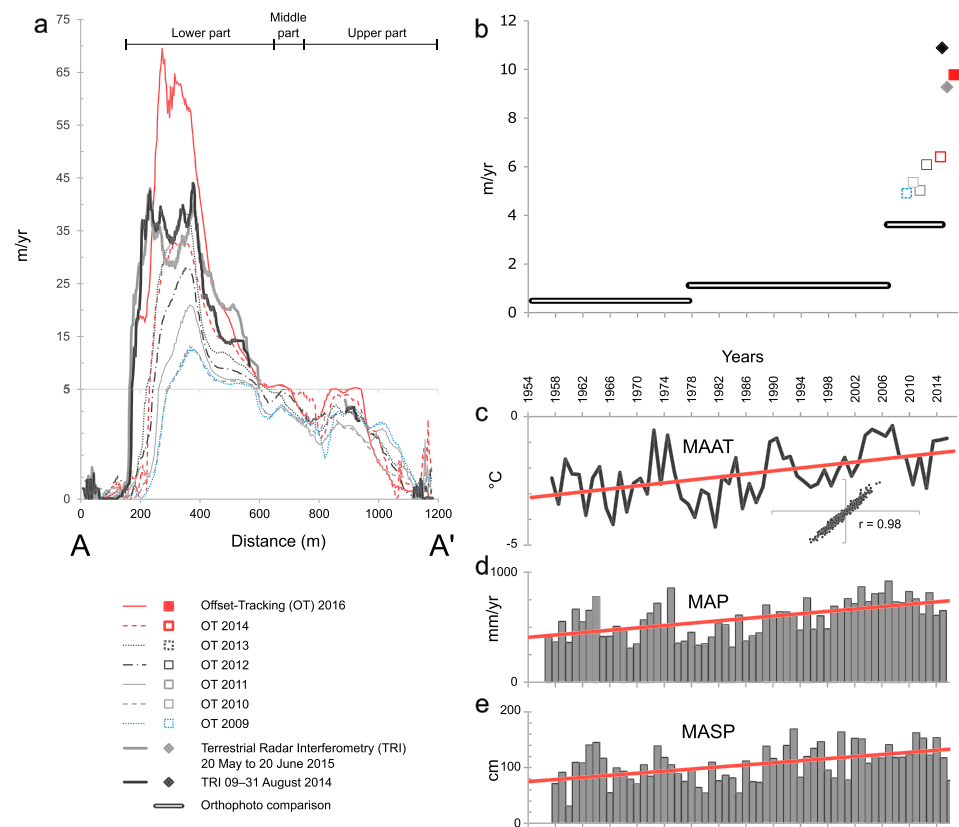


**Figure 2.** Spatial and temporal variations of displacement rates compared to modeled local climatic data for lobe A1 at Adjet. (a) Surface-parallel annual velocity in profile A-A' from offset-tracking (OT; 2009–2016, minus 2015) and Terrestrial InSAR (TRI; August 2014 and May–June 2015). Note the break in the vertical scale at  $5 \text{ myr}^{-1}$ . (b) Comparison of mean annual horizontal velocity in the direction of profile A-A' for a common area in the middle part of lobe A1 (Figure S2) from aerial feature tracking, OT, and TRI. (c) Mean annual air temperature (1954–2014). Inset shows gridded daily temperature compared to in situ logger ALT 1 (Text S2f). (d) Mean annual precipitation. (e) Maximum annual snow depth. The red lines show linear trend of climatic data from 1957 to 2016. Modeled climatic data from SeNorge.no.

parallel flow of  $\sim 69 \text{ myr}^{-1}$  in the lower part and  $\sim 5 \text{ myr}^{-1}$  in the upper part (for a visual impression see Movie S2 in the supporting information). This is an increase of 575% in the lower part and 128% in the upper, compared to velocities measured in 2009.

Surface-parallel annual velocities in profile A-A' show detailed interannual variations separating the upper part in two: (1) above and (2) below 950 m (Figure 2a). Area (1) shows general deceleration, and area (2) shows general acceleration. The middle and lower part show acceleration after a period with stable velocities in 2009 and 2010 (Figures 2a, S6, and S7). Notably, after the stable period, acceleration is delayed in the middle part (starting in 2013) with respect to the lower part.

We compare decadal displacement rates from aerial feature tracking, with single year rates from OT results and seasonal rates from TRI results, by computing the mean annual horizontal velocity in the direction of profile A-A' for a common area (Figure S2) on the lower part of lobe A1 (Figure 2b). Velocities increase at a decadal scale from  $\sim 0.5$  to  $\sim 3.6 \text{ myr}^{-1}$  from 1954 to 2014, with a recent acceleration from  $\sim 4.9$  to  $\sim 9.8 \text{ myr}^{-1}$  from 2009 to 2016. A comparison between TRI and OT confirms the recent very high velocities but highlights also that the rock glacier complex is affected by seasonal fluctuations normal for rock glaciers (Kenner et al., 2017; Figure 2b).

#### 4.2. Seasonal Trends

TRI results indicate seasonal variability of displacement rates, with higher velocities in August 2014 than in May–June 2015 (Figures 2a and 2b and S8). The accumulated LOS displacements are up to  $\sim 3.5 \text{ m}$  in



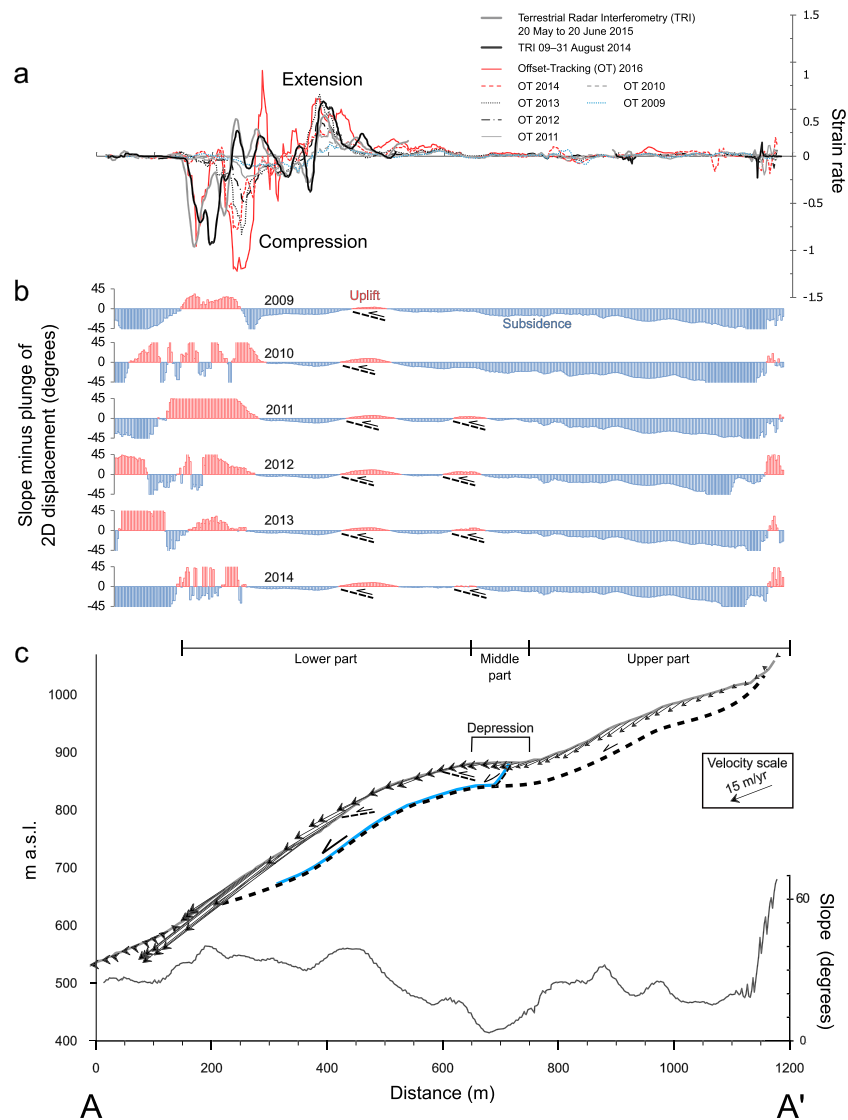


**Figure 3.** Kinematic analysis along profile A-A' in lobe A1, from offset-tracking (OT) and Terrestrial InSAR (TRI) results. (a) Spatial and temporal variations in strain rate from individual years based on surface-parallel annual velocities from OT (2009–2014) and TRI data (2014 and 2015). (b) Annual variations in uplift and subsidence calculated by subtracting slope from averaged plunge of 2-D OT surface displacement vectors. (c) Model of proposed internal structure with inferred deformation pattern, terrain surface, and slope. The vectors indicate average surface velocity and plunge from 2-D OT (2009–2014). A central depression and possible zone of elevated pore pressures (blue line) due to infiltration of water are marked. Bedrock position (dashed line) interpreted from surrounding outcrops.

23 days in August 2014 and up to ~2.7 m in 32 days in May–June 2015 (Figure S8, File S2, and Movie S1), corresponding to extrapolated mean annual velocities along the LOS of up to  $\sim 55 \text{ myr}^{-1}$  in August 2015 and  $\sim 30 \text{ myr}^{-1}$  in May–June 2015.

### 4.3. Kinematic Analysis

Based on an analysis of the strain rate along profile A-A' (Text S2e), the most noticeable kinematic signal is the pulse from extension to compression within the lower part of the rock glacier (at ~300 m from the start of profile A-A', Figure 3a). The extension increased from 2009 to 2014 in the area where the rock glacier moves over convex terrain. Further toward the front, compression has been steadily increasing from 2009 to 2014 (Figure 3a). In the low-velocity upper part, there are small-scale variations in strain rate related to slope

gradient, especially across transverse ridges and internal lobe fronts (at ~800 and ~1,050 m from the start of profile A-A'; Figure 3).

To study spatial and temporal variations, and identify the plunge of displacements, we computed 2-D vectors identified from OT results (Text S2c; Eriksen et al., 2017). Two-dimensional vectors were compared to the slope to give plunge into the ground (subsidence) and out of the ground (uplift) along profile A-A' (Figures 3b and 3c). We observe a general trend of subsidence in the upper part and alternation between uplift and subsidence in the middle and lower parts. This spatial pattern is relatively constant over time, but a new zone of uplift appears in 2011 at ~650 m from the start of the profile (Figure 3b). This uplift zone has a convex topography (slope in Figure 3c), suggesting that it is an internal lobe front. In addition, it is in an area of compression (Figure 3a), and this may therefore be the surface signal of a lobe moving over material at its front.

#### 4.4. Climatic Analysis

In situ temperature measurements (Text S2f and Figure S14) indicate permafrost conditions in the coarse blocky layer of the rock glacier lobes. Temperature measurements (362 days from August 2015 to August 2016) in fractures and cavities of the active layer at lobe A2 provided an average of  $-0.74^{\circ}\text{C}$  (logger GTL 2\_2015 at ~2.9 m depth) and an average of  $-1.92^{\circ}\text{C}$  at lobe A1 (logger GTL 3\_2015 at ~4 m depth; Figure S2 and File S3). Stable temperatures beneath snow (BTS) indicate that permafrost probably occurs in both lobes. The BTS value at logger GTL 4 (lobe A2) was  $-3.9^{\circ}\text{C}$  in February–April 2016 and  $-3.25^{\circ}\text{C}$  in February–May 2017. At logger GTL 3\_2015 (lobe A1) BTS values were more varying in 2016, ending at  $-5.2^{\circ}\text{C}$  in April, and at  $-3.75^{\circ}\text{C}$  in April 2017 (File S3). An average temperature of  $2.43^{\circ}\text{C}$  in ground surface temperatures based on 341 days (2016–2017, missing days in September) shows permafrost-free terrain in the area between the rock glacier lobes (logger GST 1), compared to an average of  $0.05^{\circ}\text{C}$  on lobe A2 (missing days in August; logger GST 1; Figure S2 and File S3).

Modeled temperature, precipitation, and snow cover data (Text S2f) indicate that climate has changed during the 62-year time span covered by the remote sensing data. Data show an increase in MAAT of  $1.8^{\circ}\text{C}$  during this period and an annual precipitation increase of 330 mm (55%). Moreover, the MASP increased by 58 cm (56%; Figures 2c–2e). If we compare the first 30 years (1957–1986) with the last 29 years (1986–2015), the MAAT has increased by  $0.91^{\circ}\text{C}$ , from  $-2.62^{\circ}\text{C}$  ( $\sigma: 0.9^{\circ}\text{C}$ ) to  $-1.71^{\circ}\text{C}$  ( $\sigma: 0.83^{\circ}\text{C}$ ). The mean annual precipitation increased with 177 mm, from 497 to 674 mm/yr from the first to the last period ( $\sigma: 142$  and  $126$  mm, respectively). Finally, the MASP increased with 33 mm, from 90 to 123 mm ( $\sigma: 33$  mm). MAAT from modeled data were compared with MAAT from in situ logger ATL 1 (Text S2f and Figures S2 and S14) and show a correlation of 0.98 (Figure 2c inset).

## 5. Discussion

The results provide information about the displacement of a rock glacier complex having rates that are comparable to advances of frozen debris lobes in Alaska (Darrow et al., 2016) and destabilized rock glaciers in the Swiss and Central Italian Alps (Delaloye et al., 2013; Scotti et al., 2016). The long time series and complementarity of methods document the temporal fluctuations of displacement rates. TRI results highlight that seasonal variations have to be considered. Seasonal variations of rock glaciers are well documented (Barsch, 1996; Haeberli, 1985; Kenner et al., 2017; Liu et al., 2013; Wirz et al., 2016). In some cases, the seasonal amplitude of the displacement is very high as, for example, in the extremely rapid Grabengufner rock glacier, which has a ratio of 1:9 between winter and summer velocities (Delaloye & Staub, 2016). Therefore, we expect that our annual displacement rates based on OT observations are overestimated. Nevertheless, the comparison of annual displacement rates from individual snow-free seasons is not affected by seasonal variations and shows a clear increasing trend.

Spatial variations in the displacement rates on the two lobes studied are well documented. The acceleration and deceleration phases in the upper part (Figure 2a) may be a consequence of irregular overloading due to rockfall and landslide activity from the highly fractured headwall, as suggested for the Grabengufner rock glacier (Delaloye et al., 2013). The results of the strain rate calculation indicate pulses from extension to compression within the lower part of the landform (Figure 3a). The increase in extension from 2009 to 2014 suggests that the rock glacier behavior is controlled by the topography and that the high velocity lower part is becoming increasingly detached from the slower upper part, as also shown for the Hinteres Langtalkar

rock glacier by Kaufmann and Ladstädter (2003) and Kaufmann and Ladstädter (2004). The reaction of the middle part is delayed compared to the fast lower part (Figure 3a). Our hypothesis is that the displacements may be taking place along internal shear zones, retrogressively propagating higher up on the rock glacier (as seen in Movie S3). Similar dynamics is described by Gorbunov et al. (1992) for the Burkutty rock glacier and by Hartl et al. (2016) for the Outer Hochebenkar rock glacier.

Velocities recorded in the lower part of the Ádjet rock glacier exceed the empirical model considered by Kääh et al. (2007) by an order of magnitude. Internal deformation of the rock glacier can be estimated using Glens' flow law of ice. The surface velocity from internal deformation is calculated using  $U_s = 2A(\rho g \sin \alpha)^3 H^4 / 4$ , where  $A$  is a rate factor depending especially on temperature,  $\rho$  is the density of the deforming material,  $g$  is the acceleration due to gravity,  $H$  is the total thickness of the deforming material, and  $\alpha$  is the surface slope averaged over  $\sim 10 H$  (e.g., Kääh et al., 2007). Following their approach further, using a maximum rock glacier thickness of 35 m, an overall density of  $\sim 2,000 \text{ kg/m}^3$  ( $\sim 40\%$  ice of density  $910 \text{ kg/m}^3$ ,  $\sim 60\%$  debris of density  $2,700 \text{ kg/m}^3$ ), a spatially averaged surface slope of  $30^\circ$  and an  $A$  value for temperate ice ( $2.1 \times 10^{-16} \text{ Pa}^{-3} \text{ a}^{-1}$ ), provides a surface velocity estimate of  $\sim 147 \text{ myr}^{-1}$  based on Glen's flow law. For reference, a more conservative  $A$  value of  $7 \times 10^{-17} \text{ Pa}^{-3} \text{ yr}^{-1}$  (adapted from Huhh1 rock glacier; Müller et al., 2016) gives a surface velocity of  $50 \text{ myr}^{-1}$ . Our recorded velocities could thus potentially stem from internal deformation alone, but it is likely that other factors contribute. In particular, the nonlinear temporal changes in velocities require other explanations. Increased displacements along shear zones may be due to meltwater percolation and increasing pore pressures (Buchli, 2016). Our calculated strain rates are above critical strain rates for crevasse formation in frozen debris (Haeberli et al., 1979) and in an isothermal ice body, water could easily percolate into the rock glacier through such structures. Similarly to destabilized rock glaciers in Mattertal (Delaloye et al., 2013), the Ádjet rock glacier moves over bedrock causing a convex break of slope. Such topography can be a controlling factor for the observed spatial pattern of extension and compression. The depression at  $\sim 700 \text{ m}$  might be related to an underlying shear zone extending toward the surface, as documented by Merz et al. (2016) from the Furggwanghorn rock glacier.

The analysis of climatic data shows a significant increase of temperature and precipitation during the 62-year period (Figures 2c–2e). From the literature, regional observed trends in permafrost temperatures in northern Scandinavia show accelerating warming since 2000 (Isaksen et al., 2007) with a change in mean annual ground temperature of between  $+0.1$  and  $+0.4 \text{ }^\circ\text{C/decade}$  (Romanovsky et al., 2016). In addition, permafrost degradation has been observed in an instrumented borehole  $\sim 30 \text{ km}$  east of Ádjet (Farbrot et al., 2013). Based on in situ measurements, climate data (since 1958), and modeling, Frauenfelder et al. (2018) found it likely that long general warming, an extreme warm summer the year before, resulted in degrading permafrost that contributed to trigger a rock avalanche in the nearby Signaldalen 26 June 2008. Combined, these results suggest increasing permafrost temperatures within the rock glacier body. Permafrost degradation may have started a positive feedback process where infiltrating water has accessed the rock glacier interior through taliks, causing energy input and hydrologic connectivity between surface and internal shear zones (Wirz et al., 2016). The increased flow velocities resulted in stretching of the permafrost body, introduced new shear zones/fractures, and enhanced percolation of water. Precipitation or melting events may then rapidly elevate pore water pressures and reduce effective stress along water-bearing shear zones (Kenner et al., 2017). Such factors might explain the observation that the lower part of the rock glacier increasingly tends to detach from the upper part. Notably, variability in seasonal displacements of the TRI results (Figures 2b and S8) and a downslope progression of TRI peak displacement from summer 2014 to spring 2015 ( $\sim 400\text{--}550 \text{ m}$  in profile A-A' Figure 2a) could be a surface signal of a progression of water pressure through such a water-bearing shear zone, as observed by Darrow et al. (2017) for frozen debris lobes in the Brooks Range of Alaska.

We have no data directly describing subsurface conditions and thermal properties for the Ádjet rock glacier complex. Nevertheless, our detailed remote sensing analysis of surface displacements gives information about areas of extension and compression possibly related to active shear zones and areas with uplift or subsidence (Figure 3). Such kinematic information provides additional details to the surface-parallel shear zone described for many alpine rock glaciers (Arenson et al., 2002; Haeberli et al., 2006) and curving shear zones found in recent results combining geophysical surveys and borehole inclinometer measurements (Merz et al., 2015).

One hypothesis is that large-scale failures due to stress release, glacio-isostatic uplift, and climate change after deglaciation  $\sim 9,100$  14C yr B.P. (ca. 10,200 cal yr B.P.; Corner, 1980; Nopper, 2015) helped form the rock glaciers. Nopper documented multiple inactive (relict) lobes between lobes A1 and A2 (Figure S18), which suggest that today's advance is not unique, but possibly part of a repeated pattern of advances controlled by variations in climatic and sediment input. Depending on the reaction to future climate forcing, variations in sediment input, and the topographic setting, failure of destabilized rock glaciers may occur (Barsch, 1996). This could have severe consequences for infrastructure and settlements in mountainous regions having a high density of creeping permafrost bodies, such as rock glaciers (Harris, 2005; Käab, 2008; Krainer et al., 2012). As permafrost landforms often are located in inaccessible, rough terrain, our remote sensing approach in conjunction with increasing availability of satellite radar data, for example, from the EU Copernicus Sentinel-1 mission, could help fulfill an urgent need to monitor the consequences of climate change (Haeberli et al., 2010). The ability to investigate large areas and to upscale site-specific geophysical and geotechnical investigations (Merz et al., 2016; Springman et al., 2012) could pave the way for an improved understanding, a more detailed characterization, and better monitoring of changes in periglacial environments.

## 6. Conclusions

Our work demonstrates the value of combining multiple remote sensing for documenting displacement of permafrost landforms. For the Ádjet rock glacier in northern Norway, we measured higher velocities and accelerations than documented in Scandinavia before. Our observations of surface displacement reveal interesting spatial and temporal kinematic patterns. In particular, two different patterns are observed, one suggesting irregular overloading in the upper part, and one possibly caused by the fast lower part progressively detaching from the slower upper part due to decreasing flow resistance. Moreover, data indicate internal kinematics as zones of compression and extension and variations in the plunge of displacement. The analysis of climatic data shows an increase of temperature and precipitation during the 62-year period, suggesting that permafrost warming with increased amounts of available water having access to internal shear zones have triggered the destabilization of the landform, but with topography as an additional control. This research is relevant for understanding the kinematics of destabilizing permafrost landforms in mountainous environments, and for improving forecasting and mitigation of future geohazards.

### Acknowledgments

TerraSAR-X satellite data were provided by DLR (projects GEO0565, GEO0764, and GEO2497). Additional data can be downloaded from <https://doi.org/10.6084/m9.figshare.5955460>. Funding for H.Ø.E. was provided by a grant (project 217720, grant RDA12/165) from Troms County Council. Development of the Norut InSAR processing chain was supported by the Norwegian Space Centre, the Research Council of Norway, and by the European Space Agency. The authors acknowledge support from Bjørn Barstad (Terratec) for preparing the orthophotos from 1954 and 1977. We are grateful to Wilfried Haeberli, Andreas Kellerer-Pirklbauer, and one anonymous reviewer whose comments clearly improved the manuscript. In addition we thank Reynald Delaloye and two anonymous reviewers for their comments on an earlier version of the manuscript. We thank Patrick Larsen, Markus Eckerstorfer, and Aleksander Amundsen for the helping during field campaigns. We are grateful to the Geological Survey of Norway for help regarding logistics, to Iselin Bakkhaug and Hannah Nopper for installing temperature loggers, and to Stein Rune Karlsen (Norut) for supplying us with tripods. We acknowledge Øyvind Ørnebakk who cleared the forest in Skibotn during the terrestrial-based radar campaigns and Tromsø Astronomy Association for letting us stay in their Skibotn Observatory during fieldwork.

### References

- Arenson, L., Hoelzle, M., & Springman, S. (2002). Borehole deformation measurements and internal structure of some rock glaciers in Switzerland. *Permafrost and Periglacial Processes*, 13(2), 117–135. <https://doi.org/10.1002/ppp.414>
- Avian, M., Kaufmann, V., & Lieb, G. K. (2005). Recent and Holocene dynamics of a rock glacier system: The example of Langtalkar (Central Alps, Austria). *Norsk Geografisk Tidsskrift*, 59(2), 149–156. <https://doi.org/10.1080/00291950510020637>
- Bakkhaug, I. (2015). Undersøkelse av ustabilit fjellparti ved Adjet, Storfjord, Troms. Betydningen av ulike kategorier av glideplan i berggrunnen og mekanismer for utglidning, Storfjord, Troms, Master Thesis, (in Norwegian). UiT-The Arctic University of Norway, pp. 126.
- Barsch, D. (1996). *Rockglaciers. Indicators for the present and former geocology in High Mountain Environments*. Heidelberg: Springer Verlag.
- Berthling, I. (2011). Beyond confusion: Rock glaciers as cryo-conditioned landforms. *Geomorphology*, 131(3–4), 98–106. <https://doi.org/10.1016/j.geomorph.2011.05.002>
- Bodin, X., Krysiacki, J.-M., Schoeneich, P., Le Roux, O., Lorier, L., Echelard, T., et al. (2016). The 2006 collapse of the Bérard rock glacier (Southern French Alps). *Permafrost and Periglacial Processes*, 28(1), 209–223. <https://doi.org/10.1002/ppp.1887>
- Buchli, T. (2016). Instabilities in Alpine permafrost: Characterisation, monitoring and modelling of active rock glaciers, (PhD thesis). ETH Zürich.
- Bunkholt, H., Redfield, T., Osmundsen, P. T., Oppikofer, T., Hermanns, R. L., & Dehls, J. (2013). The role of inherited structures in deep seated slope failures in Kåfjorden, Norway. In C. Margottini, P. Canuti, & K. Sassa (Eds.), *Landslide science and practice* (pp. 265–271). Berlin: Springer.
- Corner, G. D. (1980). Preboreal deglaciation chronology and marine limits of the Lyngen-Storfjord area, Troms, North Norway. *Boreas*, 9(4), 239–249. <https://doi.org/10.1111/j.1502-3885.1980.tb00700.x>
- Corner, G. D. (2005). Ch. 13. Scandes Mountains. In M. Seppälä (Ed.), *The physical geography of Fennoscandia, Oxford Regional Environments Series*. Oxford University Press.
- Darrow, M. M., Daanen, R. P., & Gong, W. (2017). Predicting movement using internal deformation dynamics of a landslide in permafrost. *Cold Regions Science and Technology*, 143(Supplement C), 93–104. <https://doi.org/10.1016/j.coldregions.2017.09.002>
- Darrow, M. M., Gyswy, N. L., Simpson, J. M., Daanen, R. P., & Hubbard, T. D. (2016). Frozen debris lobe morphology and movement: An overview of eight dynamic features, southern Brooks Range, Alaska. *The Cryosphere*, 10(3), 977–993. <https://doi.org/10.5194/tc-10-977-2016>
- Delaloye, R., Morard, S., Barboux, C., Abbet, D., Gruber, V., Riedo, M., & Gachet, S. (2013). Rapidly moving rock glaciers in Mattertal. In C. Graf (Ed.), *Jahrestagung der Schweizerischen Geomorphologischen Gesellschaft* (pp. 21–31).
- Delaloye, R., Perruchoud, E., Avian, M., Kaufmann, V., Bodin, X., Hausmann, H., et al. (2008). Recent interannual variations of rock glacier creep in the European Alps. *Proceeding of the Ninth International Conference on Permafrost*, (June), 343–348. <https://doi.org/10.5167/uzh-7031>



- Delaloye, R., & Staub, B. (2016). Seasonal variations of rock glacier creep: Time series observations from the Western Swiss Alps. Paper presented at the International Conference on Permafrost June 20–24, 2016, Potsdam, Germany.
- Eriksen, H. Ø. (2018). Instrumentation and temperature data (2014–2017) for the Ádjet mountain in Skibotn, Troms. Norut report 18/2018. Norut Research Institute. <http://norut.no/nb/node/6968>
- Eriksen, H. Ø., Lauknes, T. R., Larsen, Y., Corner, G. D., Bergh, S. G., Dehls, J., & Kierulf, H. P. (2017). Visualizing and interpreting surface displacement patterns on unstable slopes using multi-geometry satellite SAR interferometry (2D InSAR). *Remote Sensing of Environment*, *191*, 297–312. <https://doi.org/10.1016/j.rse.2016.12.024>
- Farbrot, H., Isaksen, K., Etzelmüller, B., & Gísnas, K. (2013). Ground thermal regime and permafrost distribution under a changing climate in northern Norway. *Permafrost and Periglacial Processes*, *24*(1), 20–38. <https://doi.org/10.1002/ppp.1763>
- Frauenfelder, R., Isaksen, K., Lato, M. J., & Noetzli, J. (2018). Ground thermal and geomechanical conditions in a permafrost-affected high-latitude rock avalanche site (Polvartinden, northern Norway). *The Cryosphere*, *12*, 1531–1550. <https://doi.org/10.5194/tc-12-1531-2018>
- Gorbunov, A. P., Titkov, S. N., & Polyakov, V. G. (1992). Dynamics of rock glaciers of the Northern Tien Shan and the Djungar Ala Tau, Kazakhstan. *Permafrost and Periglacial Processes*, *3*(1), 29–39. <https://doi.org/10.1002/ppp.3430030105>
- Haeberli, W. (1973). Die Basis Temperatur der winterlichen Schneedecke als möglicher Indikator für die Verbreitung von Permafrost. *Zeitschrift für Gletscherkunde und Glazialgeologie*, *9*(1–2), 221–227.
- Haeberli, W. (1985). Creep of mountain permafrost: Internal structure and flow of Alpine rock glaciers. Mitteilung VAW/ETHZ, 74.
- Haeberli, W., Hallet, B., Arenson, L., Elconin, R., Humlum, O., Käab, A., et al. (2006). Permafrost creep and rock glacier dynamics. *Permafrost and Periglacial Processes*, *17*(3), 189–214. <https://doi.org/10.1002/ppp.561>
- Haeberli, W., King, L., & Flotron, A. (1979). Surface movement and lichen cover studies at the active rock glacier near the Grubengletscher, Wallis, Swiss Alps. *Arctic and Alpine Research*, *11*(4), 421–441. <https://doi.org/10.2307/1550561>
- Haeberli, W., Noetzli, J., Arenson, L., Delaloye, R., Gärtner-Roer, I., Gruber, S., et al. (2010). Mountain permafrost: Development and challenges of a young research field. *Journal of Glaciology*, *56*(200), 1043–1058. <https://doi.org/10.3189/002214311796406121>
- Harris, C. (2005). Climate change, mountain permafrost degradation and geotechnical hazard. In U. M. Huber, H. K. M. Bugmann, & M. A. Reasoner (Eds.), *Global change and mountain regions: An overview of current knowledge* (pp. 215–224). Dordrecht: Springer Netherlands. [https://doi.org/10.1007/1-4020-3508-X\\_22](https://doi.org/10.1007/1-4020-3508-X_22)
- Hartl, L. E. A., Fischer, A., Stocker-Waldhuber, M., & Abermann, J. (2016). Recent speed-up of an alpine rock glacier: An updated chronology of the kinematics of outer Hochebenkar rock glacier based on geodetic measurements. *Geografiska Annaler: Series A, Physical Geography*, *98*(2), 129–141. <https://doi.org/10.1111/geoa.12127>
- Hoelzle, M. (1992). Permafrost occurrence from BTS measurements and climatic parameters in the eastern Swiss Alps. *Permafrost and Periglacial Processes*, *3*(2), 143–147.
- Ikeda, A., Matsuoka, N., & Käab, A. (2008). Fast deformation of perennially frozen debris in a warm rock glacier in the Swiss Alps: An effect of liquid water. *Journal of Geophysical Research*, *113*, F01021. <https://doi.org/10.1029/2007JF000859>
- Isaksen, K., Sollid, J. L., Holmlund, P., & Harris, C. (2007). Recent warming of mountain permafrost in Svalbard and Scandinavia. *Journal of Geophysical Research*, *112*, F02S04. <https://doi.org/10.1029/2006JF000522>
- Käab, A. (2008). Remote sensing of permafrost-related problems and hazards. *Permafrost and Periglacial Processes*, *19*(2), 107–136. <https://doi.org/10.1002/ppp.619>
- Käab, A., Frauenfelder, R., & Roer, I. (2007). On the response of rockglacier creep to surface temperature increase. *Global and Planetary Change*, *56*(1–2), 172–187. <https://doi.org/10.1016/j.gloplacha.2006.07.005>
- Käab, A., Haeberli, W., & Gudmundsson, G. H. (1997). Analysing the creep of mountain permafrost using high precision aerial photogrammetry: 25 years of monitoring Gruben rock glacier, Swiss Alps. *Permafrost and Periglacial Processes*, *8*(4), 409–426. [https://doi.org/10.1002/\(SICI\)1099-1530\(199710/12\)8:4<409::AID-PPP267>3.0.CO;2-C](https://doi.org/10.1002/(SICI)1099-1530(199710/12)8:4<409::AID-PPP267>3.0.CO;2-C)
- Kaufmann, V., & Ladstädter, R. (2003). Quantitative analysis of rock glacier creep by means of digital photogrammetry using multi-temporal aerial photographs: Two case studies in the Austrian Alps. In 8th International Conference on Permafrost. (pp. 525–530). Zurich, Switzerland.
- Kaufmann, V., & Ladstädter, R. (2004). Documentation of the movement of the Hinteres Langtalkar rock glacier abstract. In Proceedings of the 20th ISPRS Congress (6 pp.).
- Kellerer-Pirklbauer, A., & Kaufmann, V. (2012). About the relationship between rock glacier velocity and climate parameters in central Austria. *Austrian Journal of Earth Sciences*, *105*(2), 94–112.
- Kellerer-Pirklbauer, A., & Kaufmann, V. (2018). Deglaciation and its impact on permafrost and rock glacier evolution: New insight from two adjacent cirques in Austria. *Science of the Total Environment*, *621*, 1397–1414. <https://doi.org/10.1016/j.scitotenv.2017.10.087>
- Kenner, R., Phillips, M., Beutel, J., Hiller, M., Limpach, P., Pointner, E., & Volken, M. (2017). Factors controlling velocity variations at short-term, seasonal and multiyear time scales, Ritigraben rock glacier, Western Swiss Alps. *Permafrost and Periglacial Processes*, *28*(4), 675–684. <https://doi.org/10.1002/ppp.1953>
- Kraimer, K., Mussner, L., Behm, M., & Hausmann, H. (2012). Multi-disciplinary investigation of an active rock glacier in the Sella group (dolomites; northern Italy). *Austrian Journal of Earth Sciences*, *105*(2), 48–62.
- Lauknes, T. R., Shanker, A. P., Dehls, J. F., Zebker, H. A., Henderson, I. H. C., & Larsen, Y. (2010). Detailed rockslide mapping in northern Norway with small baseline and persistent scatterer interferometric SAR time series methods. *Remote Sensing of Environment*, *114*(9), 2097–2109. <https://doi.org/10.1016/j.rse.2010.04.015>
- Lilleøren, K. S., & Etzelmüller, B. (2011). A regional inventory of rock glaciers and ice-cored moraines in Norway. *Geografiska Annaler*, *93*(3), 175–191. <https://doi.org/10.1111/j.1468-0459.2011.00430.x>
- Liu, L., Millar, C. I., Westfall, R. D., & Zebker, H. A. (2013). Surface motion of active rock glaciers in the Sierra Nevada, California, USA: Inventory and a case study using InSAR. *The Cryosphere*, *7*(4), 1109–1119. <https://doi.org/10.5194/tc-7-1109-2013>
- Merz, K., Green, A. G., Buchli, T., Springman, S. M., & Maurer, H. (2015). A new 3-D thin-skinned rock glacier model based on helicopter GPR results from the Swiss Alps. *Geophysical Research Letters*, *42*, 4464–4472. <https://doi.org/10.1002/2015GL063951>
- Merz, K., Maurer, H., Rabenstein, L., Buchli, T., Springman, S. M., & Zweifel, M. (2016). Multidisciplinary geophysical investigations over an alpine rock glacier. *Geophysics*, *81*(1), WA147–WA157. <https://doi.org/10.1190/geo2015-0157.1>
- Moore, P. L. (2014). Deformation of debris-ice mixtures. *Reviews of Geophysics*, *52*(3), 435–467. <https://doi.org/10.1002/2014RG000453>
- Müller, J., Vieli, A., & Gärtner-Roer, I. (2016). Rock glaciers on the run—Understanding rock glacier landform evolution and recent changes from numerical flow modeling. *The Cryosphere*, *10*(6), 2865–2886. <https://doi.org/10.5194/tc-10-2865-2016>
- Noetzli, J., Luethi, R., & Staub, B. (2016). PERMOS 2016. Permafrost in Switzerland 2010/2011 to 2013/2014. Glaciological Report (Permafrost) No. 12-15 of the Cryospheric Commission of the Swiss Academy of Sciences, 85.
- Nopper, H. (2015). Geomorphological study of the rock-slope failure at Adjet, Storfjord, Troms, (Master thesis). (123 pp.) UiT-The Arctic University of Norway, Tromsø, Norway.

- Osmundsen, P. T., Henderson, I. H. C., Lauknes, T. R., Larsen, Y., Redfield, T. F., & Dehls, J. (2009). Active normal fault control on landscape and rock-slope failure in northern Norway. *Geology*, *37*(2), 135–138. <https://doi.org/10.1130/G25208A.1>
- Rignot, E., Hallet, B., & Fountain, A. (2002). Rock glacier surface motion in Beacon Valley, Antarctica, from synthetic-aperture radar interferometry. *Geophysical Research Letters*, *29*(12), 1607. <https://doi.org/10.1029/2001GL013494>
- Roer, I., Haeberli, W., Avian, M., Kaufmann, V., Delaloye, R., Lambiel, C., & Kääh, A. (2008). Observations and considerations on destabilizing active rock glaciers in the European Alps. Ninth International Conference on Permafrost, 2, 1505–1510.
- Roer, I., Kääh, A., & Dikau, R. (2005). Rockglacier acceleration in the Turtmann valley (Swiss Alps): Probable controls. *Norsk Geografisk Tidsskrift - Norwegian Journal of Geography*, *59*(2), 157–163. <https://doi.org/10.1080/00291950510020655>
- Romanovsky, V. E., Smith, S. L., Isaksen, K., Shiklomanov, N. I., Streletskiy, D. A., Kholodov, A. L., et al. (2016). Terrestrial permafrost [in "State of the Climate in 2015"]. *American Meteorological Society*, *97*(8), 149–152.
- Scotti, R., Crosta, G. B., & Villa, A. (2016). Destabilisation of creeping permafrost: The Plator rock glacier case study (Central Italian Alps). *Permafrost and Periglacial Processes*, *28*(1), 224–236. <https://doi.org/10.1002/ppp.1917>
- Springman, S. M., Arenson, L. U., Yamamoto, Y., Maurer, H., Kos, A., Buchli, T., & Derungs, G. (2012). Multidisciplinary investigations on three rock glaciers in the Swiss Alps: Legacies and future perspectives. *Geografiska Annaler: Series A, Physical Geography*, *94*(2), 215–243. <https://doi.org/10.1111/j.1468-0459.2012.00464.x>
- Wang, X., Liu, L., Zhao, L., Wu, T., Li, Z., & Liu, G. (2017). Mapping and inventorying active rock glaciers in the northern Tien Shan of China using satellite SAR interferometry. *The Cryosphere*, *11*(2), 997–1014. <https://doi.org/10.5194/tc-11-997-2017>
- Wirz, V., Gruber, S., Purves, R. S., Beutel, J., Gärtner-Roer, I., Gubler, S., & Vieli, A. (2016). Short-term velocity variations at three rock glaciers and their relationship with meteorological conditions. *Earth Surface Dynamics*, *4*(1), 103–123. <https://doi.org/10.5194/esurf-4-103-2016>